

## Quasiparticle Band Gaps for Ultrathin GaAs/AlAs(001) Superlattices

S. B. Zhang,<sup>(1),(a)</sup> Mark S. Hybertsen,<sup>(2)</sup> Marvin L. Cohen,<sup>(1)</sup> Steven G. Louie,<sup>(1)</sup> and D. Tomanek<sup>(1),(b)</sup>

<sup>(1)</sup> *Department of Physics, University of California*

*and Materials and Chemical Sciences Division, Lawrence Berkeley Laboratory, Berkeley, California 94720*

<sup>(2)</sup> *AT&T Bell Laboratories, 600 Mountain Avenue, Murray Hill, New Jersey 07974*

(Received 26 July 1989)

The quasiparticle band energies for  $1 \times 1$  and  $2 \times 2$  GaAs/AlAs(001) superlattices have been calculated from first principles using a self-energy approach. Both superlattices have indirect band gaps. The pseudodirect gaps at the zone center derived from folding of the Brillouin zone are larger than the direct gaps. The calculated results explain the various experimental data quantitatively. Matrix elements for optical transitions near the zone center show significant anisotropy. The effects of disorder on the observed spectra are discussed.

PACS numbers: 78.65.Fa, 73.20.Dx, 73.40.Kp

It has recently become possible to grow ultrathin superlattices  $(\text{GaAs})_n(\text{AlAs})_m$  in the (001) orientation which exhibit a degree of crystalline order and small interlayer diffusion.<sup>1</sup> Total-energy studies indicate that the superlattices are metastable.<sup>2</sup> Although superlattices with  $n, m \gtrsim 5$  are well understood, the limit of  $n, m \rightarrow 1$  poses special challenges. The repeat distance of a few monolayers is too short for the commonly used envelope-function approach, from which much of our intuition about the electronic structure of superlattices is derived, to be valid. However, traditional band-structure techniques can be used for calculating the electronic structure of these systems. Since new features such as Brillouin-zone folding are expected to make these new materials different from thick-layer superlattices, there is considerable theoretical and experimental interest in their electronic structure.<sup>3-14</sup> Despite intense scrutiny, the order of the low-lying conduction-band valleys in these ultrathin superlattices remains controversial: Theoretical calculations disagree and experimentally it is difficult to disentangle intrinsic behavior from the effects of disorder.

Electronic-structure calculations for these materials have been done in the past using the local-density-functional approach (LDA).<sup>3-5</sup> A significant difficulty with the previous calculations is that the LDA, although parameter free, does not correctly predict excited-state properties such as band dispersions and energy gaps in semiconductors. Many-body correlations arising from the electron-electron interaction must be explicitly taken into account. Here we use a first-principles self-energy approach<sup>15</sup> to determine the  $1 \times 1$  ( $n=m=1$ ) and  $2 \times 2$  GaAs/AlAs(001) superlattice band structures and we resolve the outstanding controversy surrounding the order of the conduction bands. The present self-energy approach has proven accurate in application to bulk semiconductors where the calculated gaps in the quasiparticle spectrum typically agree with experiment to an accuracy of about 0.1 eV<sup>15-17</sup> and has been applied to Si/Ge strained-layer superlattices.<sup>18</sup> We find here that the ideal  $1 \times 1$  case clearly has an indirect band gap and that

furthermore, the pseudodirect gap at the zone center (derived from a zone-folded  $X_{1c}$  state) is larger than the true direct gap. The  $2 \times 2$  superlattice shows a similar energy ordering, although the separation is smaller. This contrasts with predictions of envelope-function approach and shows that the bands in these materials are dominated by atomic-scale interactions. The results presented provide a reference point for understanding the electronic structure of the ideal ultrathin superlattices and a basis for studying the effects of disorder, transport properties, and optical properties.

The quasiparticle self-energy approach used in the present study was described in detail previously<sup>15,17</sup> and further details will be presented elsewhere.<sup>19</sup> Briefly, the lattice constant of GaAs ( $a_0 = 5.6523 \text{ \AA}$ ) is used together with an ideal GaAs/AlAs(001) structure. The slight experimental lattice mismatch, ignored here, is not expected to affect the band structure significantly.<sup>7</sup> The ground-state charge density is calculated fully self-consistently within the LDA. The eigenvalues and wave functions which enter the self-energy calculation are based on a plane-wave expansion with a 16-Ry cutoff energy. The calculated self-energy accounts for the valence-valence part of the electron-electron interaction. The effects of core-valence exchange must also be considered. These relatively small and short-range effects are estimated for the superlattices from the differences between the experimental data and present quasiparticle values for bulk GaAs and AlAs. We estimate the final uncertainty in our calculated energy gaps to be about 0.1 eV.

The appropriate Brillouin zone for the  $1 \times 1$  superlattice is illustrated in the inset of Fig. 1(a), as it is folded down from the bulk zone. One can see that  $\bar{\Gamma}$  for the superlattice contains both the  $\Gamma$  and a folded  $X_z$ ; the  $\bar{M}$  contains  $X_x$  and  $X_y$ ; the  $\bar{R}$  contains the two  $L$  points of the bulk zone. Similarly, for the  $2 \times 2$  lattice,  $\bar{\Gamma}$  includes  $\Gamma$ ,  $X_z$ , and two  $\Delta(\frac{1}{2})$  points;  $\bar{M}$  has  $X_{x,y}$  plus  $W$  points; the bulk  $L$  points are mapped to  $\bar{X}$ . The  $1 \times 1$  and  $2 \times 2$  lattices have different space groups.<sup>3,13</sup> This gives rise to an even-odd change in symmetry for zone-folded states.

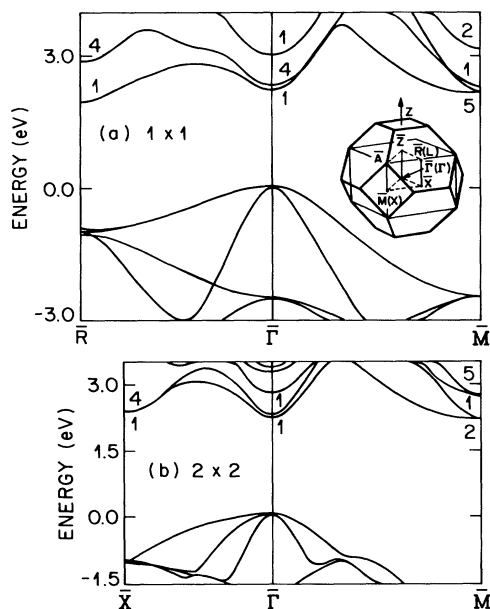


FIG. 1. Calculated quasiparticle band structure for (a)  $1 \times 1$  and (b)  $2 \times 2$  superlattices in the near gap region (excluding spin-orbit splittings). Inset: folded Brillouin zone for the  $1 \times 1$  superlattice.

The calculated quasiparticle band structures for the ultrathin superlattices are shown in Fig. 1. The important conduction-band energies relative to the valence-band edge (including the spin-orbit splitting) are collected in Table I together with results from two other recent band-structure calculations.<sup>3,4</sup> For reference, the virtual-crystal approximation (VCA) to the band structure of the  $\text{Al}_{0.5}\text{Ga}_{0.5}\text{As}$  alloy is also included (defined here as the arithmetic average of the relevant bulk energy levels). Several features of our results are important. For the  $1 \times 1$  superlattice (designations in parentheses indicate the corresponding bulk states) we note the following: (1) The conduction-band minimum is  $\bar{R}_{1c}$  ( $L_{1c}$ ) so this material has an indirect gap; (2) the  $\bar{\Gamma}_{1c}$  ( $\Gamma_{1c}$ ) state is lower than the zone-folded  $\bar{\Gamma}_{4c}$  ( $X_{1c,z}$ ) state; (3) these two  $\bar{\Gamma}$  states have different symmetry and hence do *not* mix; (4) the transverse  $\bar{M}_{5c}$  ( $X_{1c,xy}$ ) state is lower than the zone-folded  $\bar{\Gamma}_{4c}$  ( $X_{1c,z}$ ) state. For the  $2 \times 2$  superlattice: (1) The conduction-band minimum is at  $\bar{M}_{2c}$  ( $X_{1c,xy}$ ) so this material also has an indirect gap, although the separation from the  $\bar{\Gamma}_{1c}$  is sufficiently small to render this conclusion uncertain; (2) the  $\bar{\Gamma}_{1c}$  ( $\Gamma_{1c}$ ) state is still lower than the zone-folded  $\bar{\Gamma}_{1c}$  ( $X_{1c,z}$ ) state; (3) these two  $\bar{\Gamma}$  states have the *same* symmetry allowing the zone-folded state to mix with the  $\Gamma$ -derived state; (4) the  $L$ -derived  $\bar{X}_{1c}$  is now higher than the  $\bar{\Gamma}_{1c}$  and  $\bar{M}_{2c}$  states.

The indirect gap derives from a novel feature of these superlattices. A pair of equivalent bulk zone-edge states fold (Fig. 1) onto the superlattice  $\bar{M}$  (namely,  $X_x$  and  $X_y$ ) and  $\bar{R}$  ( $\bar{X}$ ) (namely,  $L$  points from  $\pm z$ ). These degenerate pairs respond differently to the superlattice po-

TABLE I. Quasiparticle energies for selected conduction-band states referenced to the top of the valence band for  $1 \times 1$  and  $2 \times 2$  superlattices and for the  $\text{Al}_{0.5}\text{Ga}_{0.5}\text{As}$  alloy in the virtual-crystal approximation (VCA) in eV. The LDA (corrected) results from the indicated calculations are included for comparison.

$1 \times 1$	$\bar{\Gamma}_{1c}$	$\bar{\Gamma}_{4c}$	$\bar{R}_{1c}$	$\bar{M}_{5c}$
Present	2.11	2.23	1.85	2.13
WZ <sup>a</sup>	2.18	2.17	1.88	2.10
GCC <sup>b</sup>	1.93	1.99	1.69	...
$2 \times 2$	$\bar{\Gamma}_{1c}$	$\bar{\Gamma}_{1c}$	$\bar{X}_{1c}$	$\bar{M}_{2c}$
Present	2.18	2.23	2.34	2.16
WZ <sup>a</sup>	2.23	2.02	2.35	2.06
GCC <sup>b</sup>	2.03	1.85	...	...
VCA	$\Gamma_{1c}$	$X_{1c,z}$	$L_{1c}$	$X_{1c,xy}$
Present	2.32	2.13	2.32	2.13

<sup>a</sup> Reference 3.

<sup>b</sup> Reference 4.

tential depending on the superlattice period (and hence the space group). These states have been designated as "segregating" states by Wei and Zunger.<sup>3</sup> A real-space picture is given in Ref. 19. Briefly, for  $n$  odd in the  $n \times n$  superlattice, the  $X_{1c}$ -derived states stick together forming the  $\bar{M}_{5c}$  doublet while the  $X_{3c}$ -derived and  $L_{1c}$ -derived states split. The latter yield the low-lying  $\bar{R}_{1c}$  conduction-band minimum for the  $1 \times 1$  superlattice. For  $n$  even, the situation is reversed. The effect is less pronounced, the splitting being due to a first neighbor rather than an on-site difference in potential. Nonetheless, this contributes to the indirect conduction-band minimum for the  $2 \times 2$  superlattice ( $\bar{M}_{2c}$ ). Note that these oscillations lead to conduction-band energies (e.g.,  $\bar{R}_{1c}$ ) quite different from the VCA prediction for the disordered  $\text{Al}_{0.5}\text{Ga}_{0.5}\text{As}$  alloy. However, the average position of the relevant doublet (e.g.,  $\bar{R}_{1c}$  and  $\bar{R}_{4c}$ ) is almost identical to the VCA result.

In contrast to the predictions of the envelope approximation as applied to larger-period superlattices, we find that the direct ( $\Gamma_{1c}$ -derived) gap is smaller than the pseudodirect ( $X_{1c,z}$ -derived) gap and the direct gap is *larger* in the  $2 \times 2$  case than in the  $1 \times 1$  case. The  $\Gamma_{1c}$ -derived state falls considerably lower than the VCA prediction for the alloy. This is a consequence of an atomic-scale localization effect (to be distinguished from confinement usually associated with thicker quantum-well systems). The more repulsive Al pseudopotentials push the charge of this excited state into the GaAs region. The effect is largest for this  $\Gamma$ -derived state which is predominantly antibonding  $s$  like on the cation site and much smaller for the interstitial  $X$ -derived states. About 65% of the  $\bar{\Gamma}_{1c}$  superlattice state is localized in the GaAs region. Since this localization is atomic in nature, it may be the cause of the large bowing effect for the  $\Gamma_{1c}$  state

(0.1–0.15 eV) observed in alloys.<sup>20</sup>

Another contribution to the order of levels at  $\bar{\Gamma}$  in the superlattices is level repulsion (between  $\bar{\Gamma}_{4c}$  and  $\bar{\Gamma}_{4b}$  in the  $1 \times 1$  superlattice and between  $\bar{\Gamma}_{1c}$  and the  $\Gamma$ -derived  $\bar{\Gamma}_{1c}$  in the  $2 \times 2$  case). There is also a difference in the many-body correction for the  $\Gamma$ - and  $X_z$ -derived states. Another interesting consequence is that the  $X_{xy}$ -derived states (e.g.,  $\bar{M}_{5c}$ ) are lower in energy than the  $X_z$ -derived state (e.g.,  $\bar{\Gamma}_{4c}$ ). This is also in contrast to the predictions of the envelope approximation for longer-period superlattices where the smaller mass for the  $X_{xy}$ -derived states along the  $z$  axis should push them higher.

Some previous calculations based on the LDA included empirical corrections to obtain band gaps of approximately the correct size (Table I).<sup>3,4</sup> In most cases, they give the  $\Gamma$ -derived  $\bar{\Gamma}_{1c}$  state above the  $X_{1c,z}$ -derived state, in contrast to the present calculation. This is partly because the many-body corrections used to correct the LDA calculations are empirically derived while the present calculation takes into account the wave functions of the superlattice directly in calculating the self-energy operator. The other reason for the discrepancy is basis-set completeness. We find that if fewer plane waves (corresponding to a cutoff of 12 Ry) are used, the order of the  $\Gamma$ - and  $X_z$ -derived states switches in the  $2 \times 2$  superlattice. It is crucial to use a complete basis here because the mixing between these two states is quite delicate.

We now compare our band structure for the ideal ultrathin superlattices to available experimental data. First consider the direct gap. For the  $1 \times 1$  lattice, a recent ellipsometry measurement gives  $E_0 = 2.07$  eV at room temperature.<sup>4</sup> The position of the strong peak in resonant Raman scattering at room temperature ranges from 2.006 (Ref. 8) to 2.108 eV (Ref. 7) and a low-temperature position of 2.095 eV (Ref. 14) has been measured. In a luminescence experiment<sup>9</sup> performed at 2 K, the excitation threshold corresponding to the direct transition is determined to be 2.214 eV. Allowing for finite-temperature effects, the direct gap at zero temperature for the  $1 \times 1$  superlattice is between 2.1 and 2.2 eV as compared to our calculated  $E_0 = 2.11$  eV. The direct gap for the  $2 \times 2$  superlattice is well determined experimentally<sup>4,9,11,14</sup> to be 2.14–2.19 eV (2.08 eV) at zero (room) temperature in good agreement with our calculated  $E_0 = 2.18$  eV. Data for indirect transitions come mainly from low-temperature photoluminescence experiments. These range from 1.89 to 2.05 eV for the  $1 \times 1$  superlattice<sup>1,10,11</sup> and from 1.97 to 2.07 eV for the  $2 \times 2$  case.<sup>1,9,11</sup> We assign these transitions for the  $1 \times 1$  superlattice to the indirect transition to  $\bar{R}$  (1.85 eV). The calculated minimum gap at  $\bar{M}$  for the  $2 \times 2$  lattice (2.16 eV) is larger than the experimental range (1.97 to 2.07 eV).

In order for the zone-folded conduction states at  $\bar{\Gamma}$  to play a significant role in the optical properties of the superlattice, they must be connected to the valence-band edge states by dipole-allowed transitions. This comes

about due to mixing with the  $\Gamma$ -derived states through the superlattice potential. We have calculated the relevant matrix elements,  $|\langle \psi_i | \mathbf{p} | \psi_j \rangle|^2$ , for transitions from the upper valence bands to the lower conduction bands near the zone center.<sup>21</sup> These results are summarized in Fig. 2(b) for transitions from the  $\bar{\Gamma}_{5v}$ -derived valence band in the  $1 \times 1$  case. The lower of the zone-folded states ( $\bar{\Gamma}_{4c}$ ) does not mix with the  $\Gamma$ -derived  $\bar{\Gamma}_{1c}$  by symmetry so the matrix element is essentially zero. The second zone-folded state has a significant oscillator strength. The situation reverses for the  $2 \times 2$  superlattice. However, the matrix element is further reduced by the spatial separation of the electrons and holes, being about 0.01 a.u. (compared to 0.25 a.u. for the  $\bar{\Gamma}_{1c}$ -derived level). Moving away from the zone center, there is a significant anisotropy in the matrix elements which derives from the anticrossing behavior in the  $k_z$  direction which is illustrated in Fig. 2(a). As the anticrossing is approached, the  $\bar{\Gamma}_{1c}$ - and  $\bar{\Gamma}_{4c}$ -derived bands exhibit strong mixing. The oscillator strength is transferred from the lower to the upper band. In the perpendicular direction, where no avoided crossing occurs, the oscillator strength for the  $\bar{\Gamma}_{1c}$ -derived band drops smoothly and the zone-folded band has very little oscillator strength.

The band structure presented here for the ultrathin superlattices is appropriate for the perfectly ordered case. In real samples, there will be reduced order caused by

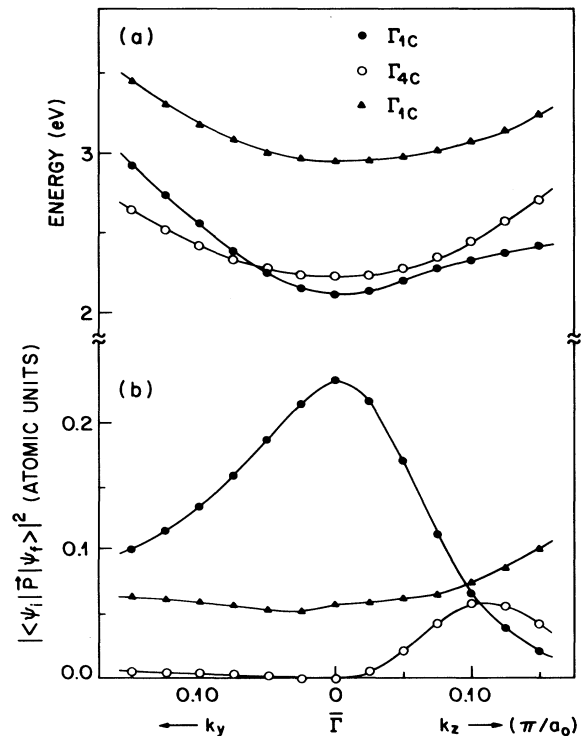


FIG. 2. Calculated (a) quasiparticle conduction-band energies, and (b) optical matrix elements squared, near the zone center for the  $1 \times 1$  superlattice.

interdiffusion and possible inhomogeneities in layer thickness. Our calculations form a basis for discussing such effects. We consider two examples here. First, the position of the measured luminescence peak for the  $2 \times 2$  superlattice is considerably below the minimum band-to-band transition in our calculation. This could easily arise from an imperfection in the growing process, e.g., the local excess of Ga or Al ions creating  $3 \times 1$  and  $1 \times 3$  regions. The direct gap for an ideal  $3 \times 1$  superlattice is calculated to be 1.87 eV which is much smaller than the calculated gap for the  $2 \times 2$  lattice. Since luminescence generally yields the lowest-energy recombination channel, even if these  $3 \times 1$  structures only form local defects, the associated recombination energy will be bounded by this 1.87 eV. Although the probability of forming relatively large local lattices is very low, the transition-matrix elements for direct transitions are much larger than those for indirect transitions. Second, claims for observation of the pseudodirect transitions must be critically reevaluated. For well-ordered samples, the pseudodirect gap is larger than the direct gap and hence does not contribute to the luminescence. Furthermore, in the  $1 \times 1$  case, the pseudodirect transitions only have significant dipole matrix elements away from the zone center near the avoided crossing. The zone-center transition is only weakly dipole allowed in the  $2 \times 2$  case. However, the discussion above makes it clear that the energy separation between the direct and pseudodirect gaps is sensitive to disorder. In the alloy, the order of the levels is reversed from the superlattices (Table I). Hence, the degree of disorder will be very important in tuning the separation between direct and pseudodirect transition energies, and even their order, as well as the degree of resonant mixing which will control the relative oscillator strength: e.g., the separation and relative strength of the peaks in recent resonant Raman experiments.<sup>14</sup> This illustrates that unambiguous experimental identification of the pseudodirect transitions is quite difficult.

The work at Berkeley was supported by National Science Foundation Grant No. DMR8818404 and by the Director, Office of Energy Research, Office of Basic Energy Sciences, Materials Sciences Division of the U.S. Department of Energy under Contract No. DE-AC03-76SF00098. D.T. was supported by the Center for Advanced Materials at the Lawrence Berkeley Laboratory. Cray computer time was provided by the NSF San Diego Supercomputer Center.

<sup>(a)</sup>Present address: Xerox Palo Alto Research Center, 3333 Coyote Hill Road, Palo Alto, CA 94304.

<sup>(b)</sup>Present address: Department of Physics and Astronomy and Center for Fundamental Materials Research, Michigan State University, East Lansing, MI 48824-1116.

<sup>1</sup>A. Ishibashi, Y. Mori, M. Itabashi, and M. Watanabe, *J. Appl. Phys.* **58**, 2691 (1985).

<sup>2</sup>D. M. Wood, S. H. Wei, and A. Zunger, *Phys. Rev. B* **37**, 1342 (1988); D. M. Bylander and L. Kleinman, *Phys. Rev. B* **34**, 5280 (1986); S. Ciraci and I. P. Batra, *Phys. Rev. Lett.* **58**, 2114 (1987).

<sup>3</sup>S. H. Wei and A. Zunger, *J. Appl. Phys.* **63**, 5794 (1988).

<sup>4</sup>M. Alouani, S. Gopalan, M. Garriga, and N. E. Christensen, *Phys. Rev. Lett.* **61**, 1643 (1988); S. Gopalan, N. E. Christensen, and M. Cardona (unpublished).

<sup>5</sup>T. Nakayama and H. Kamimura, *J. Phys. Soc. Jpn.* **54**, 4726 (1985).

<sup>6</sup>M. A. Gell, D. Ninno, M. Jaros, and D. C. Herbert, *Phys. Rev. B* **34**, 2416 (1986).

<sup>7</sup>M. Cardona, T. Suemoto, N. E. Christensen, T. Isu, and K. Ploog, *Phys. Rev. B* **36**, 5906 (1987).

<sup>8</sup>N. Kobayashi, T. Toriyama, and Y. Horikoshi, *Appl. Phys. Lett.* **50**, 1811 (1987).

<sup>9</sup>D. S. Jiang, K. Kelting, T. Isu, H. J. Queisser, and K. Ploog, *J. Appl. Phys.* **63**, 845 (1988).

<sup>10</sup>E. Finkman, M. D. Sturge, and M. C. Tamargo, *Appl. Phys. Lett.* **49**, 1299 (1986).

<sup>11</sup>J. Nagle, M. Garriga, W. Stolz, T. Isu, and K. Ploog, *J. Phys. (Paris), Colloq.* **48**, C5-495 (1987).

<sup>12</sup>G. Danan, B. Etienne, F. Mollot, R. Planel, A. M. Jean-Louis, F. Alexandre, B. Jusserand, G. Le Roux, J. Y. Marzin, H. Savary, and B. Sermage, *Phys. Rev. B* **35**, 6207 (1987).

<sup>13</sup>Y.-T. Lu and L. J. Sham, *Phys. Rev. B* **40**, 5567 (1989).

<sup>14</sup>J. Menedez, A. Pinczuk, J. P. Valladares, L. N. Pfeiffer, K. W. West, A. C. Gossard, and J. H. English (to be published).

<sup>15</sup>M. S. Hybertsen and S. G. Louie, *Phys. Rev. B* **34**, 5390 (1986); *Comments Condens. Matter Phys. B* **13**, 223 (1987).

<sup>16</sup>R. W. Godby, M. Schluter, and L. J. Sham, *Phys. Rev. B* **37**, 10159 (1988).

<sup>17</sup>S. B. Zhang, D. Tomanek, S. G. Louie, M. L. Cohen, and M. S. Hybertsen, *Phys. Rev. B* **40**, 3162 (1989).

<sup>18</sup>M. S. Hybertsen and M. Schluter, *Phys. Rev. B* **36**, 9683 (1987).

<sup>19</sup>S. B. Zhang, M. L. Cohen, S. G. Louie, D. Tomanek, and M. S. Hybertsen (unpublished).

<sup>20</sup>D. E. Aspnes, S. M. Kelso, R. A. Logan, and R. Bhatt, *J. Appl. Phys.* **60**, 754 (1986).

<sup>21</sup>The precise value is somewhat uncertain as the LDA wave functions are used to calculate the matrix elements and the self-energy calculation places the avoided crossing at a slightly different point in  $k$  space.